The Wentzel–Kramers–Brillouin Approximation for Horizontally Oriented Hexagonal Ice Crystals

M. Ibnchaikh[a], E.M. Tari[a,*], S. Zahraoui[b], A. Faké[a] and A. Bahaoui[a]

[a] *Laboratory of Theoretical Physics, Faculty of Sciences, Chouaib Doukkali University, Route Ben Mâachou, 24000, 24000 El Jadida, Morocco*
[b] *Center for Education and Training Professions, Av. Allal Al Fassi, 10000, Rabat, Morocco*

Received: 16.05.2022 & Accepted: 04.07.2022

Doi: 10.12693/APhysPolA.142.298 *e-mail: tarielmostafa@gmail.com

An analytical formulation of the Wentzel–Krame–Brillouin approximation is made for horizontally oriented hexagonal ice crystals. This work is limited to hexagonal ice columns, which have orientations with one degree of freedom. Moreover, one considers only an incidence on the flat facets. Thus, the analytical expression of the scattering amplitude form factor is determined. Finally, by numerical examples, the influence of the orientations of the particles on the scattering properties of hexagonal ice columns is shown.

topics: light scattering, Wentzel–Kramers–Brillouin approximation, form factor

1. Introduction

Non-spherical ice crystals are of great interest because of their abundance in the atmosphere. Particularly, the cirrus is composed of a large number of small particles of various shapes. The most basic and common crystals are hexagonal [1, 2]. It is known that the Mie theory can only be applied to particles with very regular shapes, such as spheres and cylinders. Extending the exact theory to other particle shapes seems to be a difficult problem. A few years ago, there were some theoretical computations and experimental studies concerning light scattering by non-spherical particles [3–6].

Nevertheless, problems of numerical instability and demands on computer resources still limit the utility of numerical techniques. Under such circumstances, the use of approximate methods becomes preferable or even mandatory. The most widely used analytical approximations for practical situations are the Rayleigh–Gans–Debye (RGD) approximation and anomalous diffraction (AD) of van de Hulst [7]. The Wentzel–Krame–Brillouin (WKB) approximation [8] is a classical approximation, which correctly takes into account the phase shift, so it does not have any restriction on the phase shift magnitude, contrary to the other approximations. The WKB approximation has been successfully applied to spheres, spheroids, and cylinders [9–12]. However, the WKB method has not been sufficiently applied for analyzing light scattering by non-spherical particles. In the last decade, some numerical studies based on the use of the WKB method have been made [13, 14]. In [15], an analytical formulation of the WKB for a hexagonal particle in a fixed orientation has been given.

In addition to the non-spherical effect of ice crystals, the orientations of these particles are also important to their optical properties. Particularly in the atmosphere, large numbers of ice particles tend to have their longest dimension oriented horizontally when they fall down [16]. It is known that hexagonal plates can have random rotational angles about their symmetry axes, which are their principal axes oriented vertically, while hexagonal columns can have orientations with one degree (1D) of freedom or two degrees (2D) of freedom. For the horizontal orientations with 1D freedom, the particles can rotate about an axis perpendicular to their principal axes. For the random orientations with 2D freedom, the columns not only rotate horizontally about an axis perpendicular to their principal axes but also rotate about their principal axes. Guang et al. [17] numerically calculated the phase functions of horizontally oriented hexagonal ice plates and columns using the finite-difference time-domain (FDTD) method. On the other hand, W. Sun and Q. Fu [18] applied the anomalous diffraction theory to study the scattering properties of arbitrarily oriented hexagonal crystals and calculated the scattering integral of extinction for ice columns that have orientations with 2D freedom.

The study of scattering properties of hexagonal ice plates, which have orientations with 1D freedom, can be done easily, as in [15], where two specific orientations of the particle for normal incidence have been analyzed (i.e., flat incident rays and edge-on incidence). But this is not the case with hexagonal ice columns, which rotate about an axis perpendicular to their principal axes. Moreover, the scattering problem becomes more complex when the particles rotate also about their principal axes.

The purpose of this paper is to develop an analytical formulation of the WKB method to derive analytical expressions of the absolute value of the amplitude form factor for horizontally oriented hexagonal ice columns. This work is limited to hexagonal ice columns, which rotate about an axis perpendicular to their principal axes (1D). Here, we only consider an incidence on the flat facets. Finally, for illustration, some numerical examples are analyzed. It can be noted that the same treatment can be repeated for the edge-on incidence.

2. Amplitude form factor of horizontally oriented hexagonal columns

A hexagonal particle is defined in terms of its side length (a) and principal axis length (l). Let us consider a laboratory coordinates system ($oxyz$), whose origin coincides with the geometric center of the hexagon. The particle is irradiated by a plane wave of wave number k ($k = \frac{2\pi}{\lambda}$, where λ is the wavelength), which is polarized in the direction of the x-axis and propagating along the z-axis. We note that the principal axis of the particle is arbitrarily oriented in the horizontal plane (xz) (Fig. 1). The angle β describes the rotation of the particle about the y-axis. From the symmetry of the hexagon, β is between and $\frac{\pi}{2}$. We choose, as an example, the origin of β when the principal axis coincides with the x-axis.

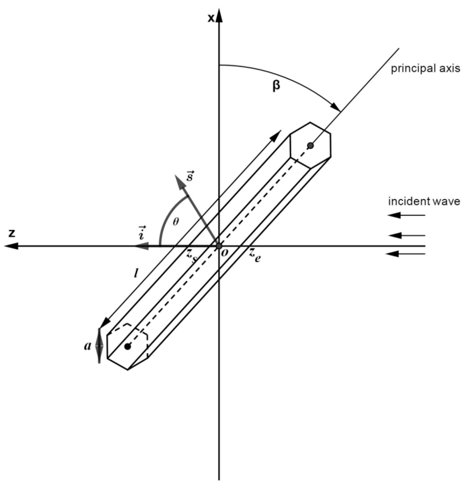

Fig. 1. Geometry of the hexagon for obliquely incidence.

The form factor for the WKB approximation is given by Klett and Sutherland [8]

$$F(\theta,\varphi) = \frac{1}{v}\int \mathrm{d}v\, \mathrm{e}^{\mathrm{i}k\boldsymbol{r}\,(\boldsymbol{i}-\boldsymbol{s})}\,\mathrm{e}^{\mathrm{i}kw}, \tag{1}$$

where v is the volume of the particle, $\boldsymbol{r}$ is a vector position of any point inside the particle, and $\boldsymbol{i}$ and $\boldsymbol{s}$ are, respectively, the unit vectors of the incident and scattered wave, θ is the scattering zenith angle, and φ is the scattering azimuthal angle. In (1), w is the optical path introduced by the scatterer, which is defined by

$$w = \int_{z_e}^{z} \mathrm{d}z' \left[m\left(z'\right) - 1\right]. \tag{2}$$

For homogeneous particle

$$w = (m-1)\left(z - z_e\right), \tag{3}$$

where m is the relative complex refractive index and z_e is the z-coordinate of the initial position of penetration of the light through the object ($z_e < 0$) (see Fig. 1).

So, (1) can be written as

$$F(\theta,\varphi) = \iiint_v \mathrm{d}x\,\mathrm{d}y\,\mathrm{d}z\, \mathrm{e}^{-\mathrm{i}kx\sin(\theta)\cos(\varphi)} \times \mathrm{e}^{-\mathrm{i}ky\sin(\theta)\sin(\varphi)}\,\mathrm{e}^{\mathrm{i}kz(m-\cos(\theta))}\,\mathrm{e}^{-\mathrm{i}kz_e(m-1)}. \tag{4}$$

After the integration of (4) on the variable z from z_e to z_s, one find

$$F(\theta,\varphi) = \frac{1}{\mathrm{i}k\big(m-\cos(\theta)\big)}\iint \mathrm{d}x\,\mathrm{d}y\, G(z_e z_s) \times \mathrm{e}^{-\mathrm{i}ky\sin(\theta)\sin(\varphi)}\,\mathrm{e}^{-\mathrm{i}kx\sin(\theta)\cos(\varphi)} \tag{5}$$

with

$$G(z_e, z_s) = \mathrm{e}^{\mathrm{i}k(m-\cos(\theta))z_s}\,\mathrm{e}^{-\mathrm{i}k(m-1)z_e} - \mathrm{e}^{\mathrm{i}k(1-\cos(\theta))z_e}, \tag{6}$$

where z_s is the z-coordinate of the intersection of the incident light and the output surface. Note that the factor $\frac{1}{v}$ is omitted.

So, for flat incident rays, the base of the hexagon is divided into three areas by the rays 1–4 (Fig. 2a). The paths in each area are a function of the variable y and are denoted by (l_n) with $n = 1, 2, 3$. Next, the hexagon is cut into thin longitudinal slices of height (l) with thickness dy and width (l_n) (Fig. 2b). The cut is made along the direction of incidence.

With the aid of the results in Fig. 2a, we measured the paths l_1, l_2, and l_3 in each area. Therefore, we have

$$\begin{cases} l_1(y) = 2\sqrt{3}\,(a+y)\,; & -a \le y \le -a/2, \\ l_2(y) = l_1(-y)\,; & a/2 \le y \le a, \\ l_3 = a\sqrt{3}; & -a/2 \le y \le a/2. \end{cases} \tag{7}$$

Furthermore, for a given β, we have two types of slices, i.e., a slice with $l_n \le l\cot(\beta)$ (Fig. 3a) and a slice with $l_n > l\cot(\beta)$ (Fig. 3b). The slices are then divided into three areas by the rays 1–4.

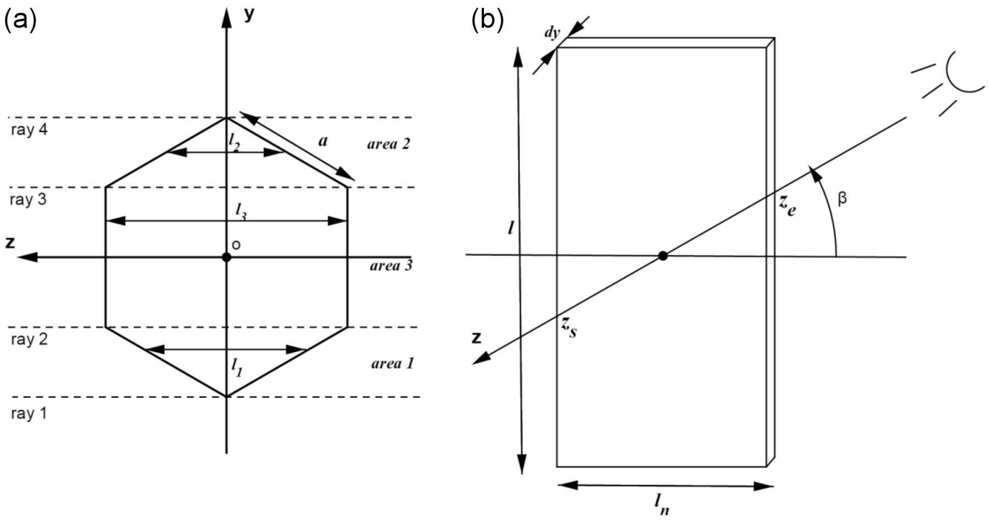

Fig. 2. (a) Geometry of cuts on the base of the hexagon for an incidence on the flat facet. (b) The slices of the hexagon are cut into three regions according to the direction of incidence.

So, we can determine the function $G(z_e, z_s)$ defined in (6) for each area, and then integrate it over the variable x to obtain the contributions from these slices to the form factor $F(\theta, \varphi)$. For the sake of brevity and clarity, we only show how to find the contribution of the slice with $l_n \le l\cot(\beta)$. Therefore, we have

$$\begin{cases} z_{e1} = -\frac{l_n}{2\cos(\beta)} - x\tan(\beta) \\ z_{s1} = \frac{l}{2\sin(\beta)} + x\cot(\beta) \end{cases}; \quad -x_N \le x \le -x_C; \tag{8}$$

$$\begin{cases} z_{e2} = -\frac{l}{2\sin(\beta)} + x\cot(\beta) \\ z_{s2} = \frac{l_n}{2\cos(\beta)} - x\tan(\beta) \end{cases}; \quad x_C \le x \le x_N; \tag{9}$$

and

$$\begin{cases} z_{e3} = -\frac{l_n}{2\cos(\beta)} - x\tan(\beta) \\ z_{s3} = \frac{l_n}{2\cos(\beta)} - x\tan(\beta) \end{cases}; \quad -x_C \le x \le x_C; \tag{10}$$

with

$$x_C = \frac{l}{2}\cos(\beta) - \frac{l_n}{2}\sin(\beta) \tag{11}$$

and

$$x_N = \frac{l}{2}\cos(\beta) + \frac{l_n}{2}\sin(\beta). \tag{12}$$

By substituting the values of z_{ej} and z_{sj} in (6) (where $j = 1, 2, 3$), one obtains the contribution of the slice, denoted as

$$f^1(\theta, \varphi, l_n)\,\mathrm{d}y = \frac{s_1+s_2+s_3}{\mathrm{i}k\big(m-\cos(\theta)\big)}\,\mathrm{e}^{-\mathrm{i}ky\sin(\theta)\sin(\varphi)}\,\mathrm{d}y, \tag{13}$$

where

$$s_1 = s_1(\theta, \varphi, l_n) = \int_{-x_N}^{-x_C} \mathrm{d}x\, G(z_{e1}, z_{s1})\,\mathrm{e}^{-\mathrm{i}kx\sin(\theta)\cos(\varphi)}, \tag{14}$$

$$s_2 = s_2(\theta, \varphi, l_n) = \int_{x_C}^{x_N} \mathrm{d}x\, G(z_{e2}, z_{s2})\,\mathrm{e}^{-\mathrm{i}kx\sin(\theta)\cos(\varphi)}, \tag{15}$$

and

$$s_3 = s_3(\theta, \varphi, l_n) = \int_{-x_C}^{x_C} \mathrm{d}x\, G(z_{e3}, z_{s3})\,\mathrm{e}^{-\mathrm{i}kx\sin(\theta)\cos(\varphi)}. \tag{16}$$

In (13), s_1, s_2, and s_3 are the contributions of each area.

The final results are rearranged as follows

$$s_1 = l_n\sin(\beta)\,\mathrm{e}^{\mathrm{i}k\frac{l}{2}A}\,\mathrm{e}^{\mathrm{i}k\frac{l_n}{2}B}\left[\frac{\mathrm{e}^{-\mathrm{i}kl_n\left(B-\frac{m-1}{\cos(\beta)}\right)}-1}{(-\mathrm{i}k\,l_n)\left(B-\frac{m-1}{\cos(\beta)}\right)} - \frac{\mathrm{e}^{-\mathrm{i}kl_nA\tan(\beta)}-1}{(-\mathrm{i}kl_nA)\tan(\beta)}\right], \tag{17}$$

$$s_2 = l_n\sin(\beta)\,\mathrm{e}^{-\mathrm{i}k\frac{l}{2}A}\,\mathrm{e}^{\mathrm{i}k\frac{l_n}{2}B}\left[\mathrm{e}^{\mathrm{i}kl_n\frac{m-\cos(\theta)}{\cos(\beta)}}\,\frac{\mathrm{e}^{-\mathrm{i}kl_n\left(B+\frac{m-\cos(\theta)}{\cos(\beta)}\right)}-1}{(-\mathrm{i}kl_n)\left(B+\frac{m-\cos(\theta)}{\cos(\beta)}\right)} - \frac{\mathrm{e}^{-\mathrm{i}kl_nB}-1}{(-\mathrm{i}kl_nB)}\right], \tag{18}$$

and

$$s_3 = \Big(l\cos(\beta) - l_n\sin(\beta)\Big)\,\mathrm{e}^{-\mathrm{i}k\frac{l}{2}A}\,\mathrm{e}^{\mathrm{i}k\frac{l_n}{2}B}\,\frac{\left[\mathrm{e}^{\mathrm{i}kl_n\frac{m-\cos(\theta)}{\cos(\beta)}}-1\right]\left[\mathrm{e}^{-\mathrm{i}k\left(l_n\tan(\beta)-l\right)A}-1\right]}{(-\mathrm{i}k)\big(l_n\tan(\beta)-l\big)A} \tag{19}$$

with

$$A = \cos(\beta)\sin(\theta)\cos(\varphi) + \big(1 - \cos(\theta)\big)\sin(\beta) \tag{20}$$

and

$$B = \sin(\beta)\sin(\theta)\cos(\varphi) - \big(1 - \cos(\theta)\big)\cos(\beta). \tag{21}$$

We note that for the normal incidence ($\beta = 0$), the parameters s_1 and s_2 vanish.

The same processing is repeated for the slice with $l_n > l\cot(\beta)$. The contribution from this slice to the form factor is given by

$$f^2(\theta,\varphi,l_n)\,\mathrm{d}y = \frac{s_1' + s_2' + s_3'}{\mathrm{i}k\big(m - \cos(\theta)\big)}\,\mathrm{e}^{-\mathrm{i}ky\sin(\theta)\sin(\varphi)}\,\mathrm{d}y, \tag{22}$$

where

$$s_1' = s_1'(\theta,\varphi,l_n) = s_{10}'\,\mathrm{e}^{\mathrm{i}k\,l_n B/2}, \tag{23}$$

$$s_2' = s_2'(\theta,\varphi,l_n) = s_{20}'\,\mathrm{e}^{-\mathrm{i}k\,l_n B/2}, \tag{24}$$

and

$$s_3' = s_3'(\theta,\varphi,l_n) = \Big(l_n\sin(\beta) - l\cos(\beta)\Big)\,\mathrm{e}^{-\mathrm{i}k\frac{l}{2}A}\,\mathrm{e}^{\mathrm{i}k\frac{l_n}{2}B}\,\frac{\Big[\mathrm{e}^{\mathrm{i}kl\frac{m-\cos(\theta)}{\sin(\beta)}} - 1\Big]\Big[\mathrm{e}^{-\mathrm{i}k(l_n - l\cot(\beta))B} - 1\Big]}{(-\mathrm{i}k)\big(l_n - l\cot(\beta)\big)B} \tag{25}$$

with

$$s_{10}' = l\cos(\beta)\left[\mathrm{e}^{\mathrm{i}k\frac{l}{2}\frac{m-\cos(\theta)}{\sin(\beta)}}\,\frac{\sin\Big(k\frac{l}{2}\big(A - \frac{m-\cos(\theta)}{\sin(\beta)}\big)\Big)}{k\frac{l}{2}\big(A - \frac{m-\cos(\theta)}{\sin(\beta)}\big)} - \frac{\sin\big(k\frac{l}{2}A\big)}{k\frac{l}{2}A}\right] \tag{26}$$

and

$$s_{20}' = l\cos(\beta)\left[\mathrm{e}^{\mathrm{i}k\frac{l}{2}(\frac{m-1}{\sin(\beta)})}\,\frac{\sin\Big(k\frac{l}{2}\big(A + \frac{m-1}{\sin(\beta)}\big)\Big)}{k\frac{l}{2}\big(A + \frac{m-1}{\sin(\beta)}\big)} - \mathrm{e}^{-\mathrm{i}k\frac{l}{2}\frac{1-\cos\theta}{\sin(\beta)}}\,\frac{\sin\big(k\frac{l}{2}B\big)\cot(\beta)}{k\frac{l}{2}B\cot(\beta)}\right] \tag{27}$$

It can be seen that parameters s_1' and s_2' vanish when $\beta = \frac{\pi}{2}$.

Integrating the contributions from all slices over y, we obtain the form factor in the forms

$$F_{\text{flat}}(\theta,\varphi,\beta) = \begin{cases} H_1 + H_3 + H_2; \\ \quad \text{for } 0 \le \beta \le \arctan\left(\frac{l}{a\sqrt{3}}\right) \\ H_1^1 + H_1^2 + H_3^2 + H_2^2 + H_2^1; \\ \quad \text{for } \arctan\left(\frac{l}{a\sqrt{3}}\right) < \beta \end{cases} \tag{28}$$

where

$$H_1 = H_1(\theta,\varphi,\beta) = \int_{-a}^{-\frac{a}{2}} \mathrm{d}y\, f^1(\theta,\varphi,l_1(y)), \tag{29}$$

$$H_2 = H_2(\theta,\varphi,\beta) = \int_{\frac{a}{2}}^{a} \mathrm{d}y\, f^1(\theta,\varphi,l_2(y)), \tag{30}$$

$$H_3 = H_3(\theta,\varphi,\beta) = \int_{-\frac{a}{2}}^{\frac{a}{2}} \mathrm{d}y\, f^1(\theta,\varphi,l_3), \tag{31}$$

$$H_1^1 = H_1^1(\theta,\varphi,\beta) = \int_{-a}^{-y_1} \mathrm{d}y\, f^1(\theta,\varphi,l_1(y)), \tag{32}$$

$$H_2^1 = H_2^1(\theta,\varphi,\beta) = \int_{y_1}^{a} \mathrm{d}y\, f^1(\theta,\varphi,l_2(y)), \tag{33}$$

$$H_1^2 = H_1^2(\theta,\varphi,\beta) = \int_{-y_1}^{-\frac{a}{2}} \mathrm{d}y\, f^2(\theta,\varphi,l_1(y)), \tag{34}$$

$$H_2^2 = H_2^2(\theta,\varphi,\beta) = \int_{\frac{a}{2}}^{y_1} \mathrm{d}y\, f^2(\theta,\varphi,l_2(y)), \tag{35}$$

$$H_3^2 = H_3^2(\theta,\varphi,\beta) = \int_{-\frac{a}{2}}^{\frac{a}{2}} \mathrm{d}y\, f^2(\theta,\varphi,l_3) \tag{36}$$

with the limiting value of y for each area is $y_1 = a - \frac{l}{2\sqrt{3}}\cot(\beta)$.

It should be noted that the integration of these contributions over y for the normal incidence ($\beta = 0$) and for incident rays perpendicular to the base of the hexagon ($\beta = \frac{\pi}{2}$) can be done easily. The results found for the normal incidence are the same as those existing in [15]. It can also be noted that the parameters A and B (see (20) and (21)) which are introduced in (13) and (22) play an important role in determining analytical results of the form factor, because these two parameters can take the value of zero for certain values of the angles θ, φ, and β. Therefore, (13) and (22) must be simplified before integrating over y. On the other hand, it can be seen from (20) and (21) that $A = B = 0$ when $\theta = 0$. Therefore, the integration over y must be done separately at $\theta = 0$ and at $\theta \neq 0$.

Only the contributions H_3 and H_3^2 can be directly integrated using (13) and (22), because the path l_3 ($l_3 = a\sqrt{3}$) does not depend on the variable y. So, we have

$$H_3(\theta,\varphi,\beta) = d\big[s_1(\theta,\varphi,l_3) + s_2(\theta,\varphi,l_3) + s_3(\theta,\varphi,l_3)\big] \tag{37}$$

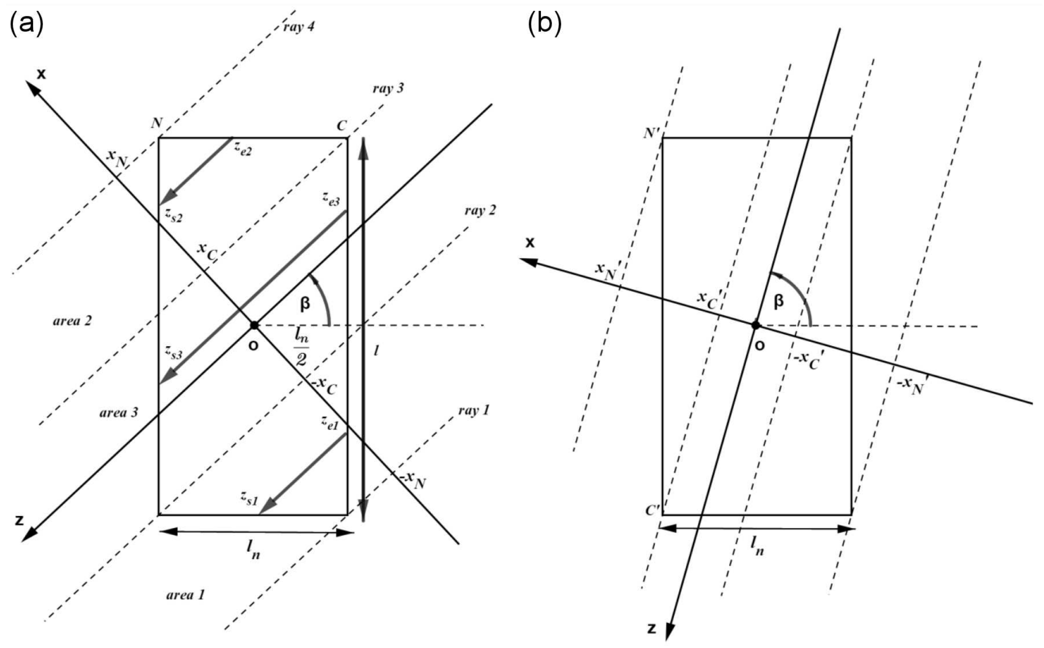

Fig. 3. Description of slices: (a) slices with $l_n \leq l\cot(\beta)$, (b) slices with $l_n > l\cot(\beta)$.

and

$$H_3^2(\theta,\varphi,\beta)=d\big[s_1'(\theta,\varphi,l_3)+s_2'(\theta,\varphi,l_3)+s_3'(\theta,\varphi,l_3)\big], \tag{38}$$

where

$$d = \frac{a}{\mathrm{i}k\,(m-\cos(\theta))}\,\frac{\sin\left(\frac{ka}{2}\right)\sin(\theta)\sin(\varphi)}{\frac{ka}{2}\sin(\theta)\sin(\varphi)}. \tag{39}$$

The values of s_1, s_2, s_3, s_1', s_2', and s_3' are obtained from (17), (18), (19), (23), (24), and (25), respectively.

In the next subsection (2.1), we begin by integrating contributions $H_1, H_2, H_1^1, H_1^2, H_2^2$, and H_2^1 over y for $\theta = 0$.

2.1. Case of $\theta = 0$

In this case, the expressions of the form factor (see (28)) are reduced to

$$F_{\text{flat}}(0,0,\beta) = \begin{cases} 2H_1(0,0,\beta) + H_3(0,0,\beta); \\ \quad \text{for } 0 \leq \beta \leq \arctan\left(\frac{l}{a\sqrt{3}}\right) \\ 2H_1^1(0,0,\beta) + 2H_1^2(0,0,\beta) \\ \quad +H_3^2(0,0,\beta); \\ \quad \text{for } \arctan\left(\frac{l}{a\sqrt{3}}\right) < \beta \end{cases} \tag{40}$$

After simplifying (13) and (22) for $A = B = 0$, the final results will be expressed as

$$H_1 = \frac{a^2\sqrt{3}}{\mathrm{i}\rho_1}\left[\left(\frac{3a\sqrt{3}\tan(\beta)}{\mathrm{i}2\rho_1} + \frac{l}{2} - \frac{a\sqrt{3}\tan(\beta)}{2}\right) \times\left(\frac{\mathrm{e}^{\mathrm{i}\rho_1}-1}{\mathrm{i}\rho_1}-1\right) - \frac{3a\sqrt{3}\tan(\beta)}{4}\right], \tag{41}$$

$$H_1^1 = \frac{l^2\sqrt{3}}{2\,\mathrm{i}\rho_1'}\cot^2(\beta)\left[\frac{l}{\mathrm{i}\rho_1'}\left(\frac{\mathrm{e}^{\mathrm{i}\rho_1'}-1}{\mathrm{i}\rho_1'}-1\right) - \frac{l}{2}\right], \tag{42}$$

and

$$H_1^2 = \frac{al\left(1-\frac{l\cot(\beta)}{a\sqrt{3}}\right)}{2}\left[\left(\frac{2l\cot(\beta)}{\mathrm{i}\rho_1'} + \frac{a\sqrt{3}}{2} - \frac{l\cot(\beta)}{2}\right) \times\left(\frac{\mathrm{e}^{\mathrm{i}\rho_1'}-1}{\mathrm{i}\rho_1'}-1\right) + \frac{a\sqrt{3}}{2} - \frac{l\cot(\beta)}{2}\right] \tag{43}$$

with

$$\rho_1 = \frac{ka\sqrt{3}}{\cos(\beta)}\,(m-1) \tag{44}$$

and

$$\rho_1' = \frac{kl}{\sin(\beta)}\,(m-1)\,. \tag{45}$$

2.2. Case of $\theta \neq 0$

In this case, we give the results of the integration of contributions $H_1, H_2, H_1^1, H_1^2, H_2^2$, and H_2^1 over y when both A and B are different from zero. The two particular cases of ($A = 0$ and $B \neq 0$) and ($A \neq 0$ and $B = 0$) can be easily deduced from the general case.

So, after rearrangement of terms of (13) and (22), these contributions can be written as follows

$$C_1 = \left[\frac{\mathrm{i}\sin(\beta)}{k\left(B-\frac{m-1}{\cos(\beta)}\right)} - \frac{\mathrm{i}\cos(\beta)}{kA}\right]\mathrm{e}^{\mathrm{i}k\frac{l}{2}A}, \tag{46}$$

$$C_2 = \left[\frac{\mathrm{i}\sin(\beta)}{k\left(B+\frac{m-\cos(\theta)}{\cos(\beta)}\right)} - \frac{\mathrm{i}\sin(\beta)}{kB}\right]\mathrm{e}^{-\mathrm{i}k\frac{l}{2}A}, \tag{47}$$

$$C_3 = \left[\frac{\mathrm{i}\cos(\beta)}{kA} - \frac{\mathrm{i}\sin(\beta)}{k\left(B+\frac{m-\cos(\theta)}{\cos(\beta)}\right)}\right]\mathrm{e}^{-\mathrm{i}k\frac{l}{2}A}, \tag{48}$$

$$C_4 = \left[\frac{\mathrm{i}\sin(\beta)}{kB} - \frac{\mathrm{i}\cos(\beta)}{kA}\right] \mathrm{e}^{-\mathrm{i}\,k\frac{l}{2}A} - C_1, \quad (49)$$

and

$$C_5 = \frac{\mathrm{i}\sin(\beta)}{kB}\left[\mathrm{e}^{\mathrm{i}\,kl\frac{(m-\cos(\theta))}{\sin(\beta)}} - 1\right] \mathrm{e}^{-\mathrm{i}\,k\,\frac{l}{2}A}. \quad (50)$$

Thus,

$$H_1 + H_2 = \frac{1}{\mathrm{i}\,k\big(m-\cos(\theta)\big)}\Big[C_1(a_1+a_2) + C_2(b_1+b_2) + C_3(d_1+d_2) + C_4(e_1+e_2)\Big], \quad (51)$$

$$H_1^1 + H_2^1 = \frac{1}{\mathrm{i}\,k\big(m-\cos(\theta)\big)}\Big[C_1(a_1^1+a_2^1) + C_2(b_1^1+b_2^1) + C_3(d_1^1+d_2^1) + C_4(e_1^1+e_2^1)\Big], \quad (52)$$

and

$$H_1^2 + H_2^2 = \frac{1}{\mathrm{i}\,k\big(m-\cos(\theta)\big)}\left[\left(S'_{10}-C_5\right)\left(a_1^2+a_2^2\right) + \left(S'_{20}+C_5\,\mathrm{e}^{\mathrm{i}\,klB\cot(\beta)}\right)\left(b_1^2+b_2^2\right)\right], \quad (53)$$

where

$$a_1 = \int_{-a}^{-\frac{a}{2}} \mathrm{d}y\,\mathcal{K}^*(\theta,\varphi)\,\mathrm{e}^{\mathrm{i}\,k\left(\frac{m-1}{\cos(\beta)}-\frac{B}{2}\right)l_1(y)}, \quad (54)$$

$$a_2 = \int_{\frac{a}{2}}^{a} \mathrm{d}y\,\mathcal{K}^*(\theta,\varphi)\,\mathrm{e}^{\mathrm{i}\,k\left(\frac{m-1}{\cos(\beta)}-\frac{B}{2}\right)l_2(y)}, \quad (55)$$

with $\mathcal{K} = \mathrm{e}^{\mathrm{i}\,ky\sin(\theta)\sin(\varphi)}$ and

$$b_1 = \int_{-a}^{-\frac{a}{2}} \mathrm{d}y\,\mathcal{K}^*(\theta,\varphi)\,\mathrm{e}^{-\mathrm{i}\,k\frac{B}{2}l_1(y)}, \quad (56)$$

$$b_2 = \int_{\frac{a}{2}}^{a} \mathrm{d}y\,\mathcal{K}^*(\theta,\varphi)\,\mathrm{e}^{-\mathrm{i}\,k\frac{B}{2}l_2(y)}, \quad (57)$$

$$d_1 = \int_{-a}^{-\frac{a}{2}} \mathrm{d}y\,\mathcal{K}^*(\theta,\varphi)\,\mathrm{e}^{\mathrm{i}\,k\left(\frac{m-\cos(\theta)}{\cos(\beta)}+\frac{B}{2}\right)l_1(y)}, \quad (58)$$

$$d_2 = \int_{\frac{a}{2}}^{a} \mathrm{d}y\,\mathcal{K}^*(\theta,\varphi)\,\mathrm{e}^{\mathrm{i}\,k\left(\frac{m-\cos(\theta)}{\cos(\beta)}+\frac{B}{2}\right)l_2(y)}, \quad (59)$$

$$e_1 = \int_{-a}^{-\frac{a}{2}} \mathrm{d}y\,\mathcal{K}^*(\theta,\varphi)\,\mathrm{e}^{\mathrm{i}\,k\frac{B}{2}l_1(y)}, \quad (60)$$

$$e_2 = \int_{\frac{a}{2}}^{a} \mathrm{d}y\,\mathcal{K}^*(\theta,\varphi)\,\mathrm{e}^{\mathrm{i}\,k\frac{B}{2}l_2(y)}, \quad (61)$$

$$a_1^1 = \int_{-a}^{-y_1} \mathrm{d}y\,\mathcal{K}^*(\theta,\varphi)\,\mathrm{e}^{\mathrm{i}\,k\left(\frac{m-1}{\cos(\beta)}-\frac{B}{2}\right)l_1(y)}, \quad (62)$$

$$a_2^1 = \int_{y_1}^{a} \mathrm{d}y\,\mathcal{K}^*(\theta,\varphi)\,\mathrm{e}^{\mathrm{i}\,k\left(\frac{m-1}{\cos(\beta)}-\frac{B}{2}\right)l_2(y)}, \quad (63)$$

$$b_1^1 = \int_{-a}^{-y_1} \mathrm{d}y\,\mathcal{K}^*(\theta,\varphi)\,\mathrm{e}^{-\mathrm{i}\,k\frac{B}{2}l_1(y)}, \quad (64)$$

$$b_2^1 = \int_{y_1}^{a} \mathrm{d}y\,\mathcal{K}^*(\theta,\varphi)\,\mathrm{e}^{-\mathrm{i}\,k\frac{B}{2}l_2(y)}, \quad (65)$$

$$d_1^1 = \int_{-a}^{-y_1} \mathrm{d}y\,\mathcal{K}^*(\theta,\varphi)\,\mathrm{e}^{\mathrm{i}\,k\left(\frac{m-\cos(\theta)}{\cos(\beta)}+\frac{B}{2}\right)l_1(y)}, \quad (66)$$

$$d_2^1 = \int_{y_1}^{a} \mathrm{d}y\,\mathcal{K}^*(\theta,\varphi)\,\mathrm{e}^{\mathrm{i}\,k\left(\frac{m-\cos(\theta)}{\cos(\beta)}+\frac{B}{2}\right)l_2(y)}, \quad (67)$$

$$e_1^1 = \int_{-a}^{-y_1} \mathrm{d}y\,\mathcal{K}^*(\theta,\varphi)\,\mathrm{e}^{\mathrm{i}\,k\frac{B}{2}l_1(y)}, \quad (68)$$

$$e_2^1 = \int_{y_1}^{a} \mathrm{d}y\,\mathcal{K}^*(\theta,\varphi)\,\mathrm{e}^{\mathrm{i}\,k\frac{B}{2}l_2(y)}, \quad (69)$$

$$a_1^2 = \int_{-y_1}^{-\frac{a}{2}} \mathrm{d}y\,\mathcal{K}^*(\theta,\varphi)\,\mathrm{e}^{\mathrm{i}\,k\frac{B}{2}l_1(y)}, \quad (70)$$

$$a_2^2 = \int_{a/2}^{y_1} \mathrm{d}y\,\mathcal{K}^*(\theta,\varphi)\,\mathrm{e}^{\mathrm{i}\,k\frac{B}{2}l_2(y)}, \quad (71)$$

$$b_1^2 = \int_{-y_1}^{-\frac{a}{2}} \mathrm{d}y\,\mathcal{K}^*(\theta,\varphi)\,\mathrm{e}^{-\mathrm{i}\,k\frac{B}{2}l_1(y)}, \quad (72)$$

$$b_2^2 = \int_{\frac{a}{2}}^{y_1} \mathrm{d}y\,\mathcal{K}^*(\theta,\varphi)\,\mathrm{e}^{-\mathrm{i}\,k\frac{B}{2}l_2(y)}. \quad (73)$$

It is clear that by changing the variables, the parameters of index 2 can be easily deduced from those of index 1 because we have $l_2(y) = l_1(-y)$.

We denote

$$u_1 = \frac{\sqrt{3}ka}{\cos(\beta)}\big(m-\cos(\theta)\big), \quad (74)$$

$$v_1 = \frac{ka}{2}\sin(\theta)\sin(\varphi), \quad (75)$$

$$q_1 = \frac{\sqrt{3}ka}{2}B, \quad (76)$$

$$u_1^{'} = \frac{kl}{\sin(\beta)}\big(m-\cos(\theta)\big), \quad (77)$$

$$v_1^{'} = \frac{l\cot(\beta)}{a\sqrt{3}}\,v_1, \quad (78)$$

$$q_1^{'} = \frac{l\cot(\beta)}{a\sqrt{3}}\,q_1. \quad (79)$$

Thus,

$$a_1 = \frac{a}{2}\,\mathrm{e}^{\mathrm{i}\,2v_1}\,\frac{\mathrm{e}^{\mathrm{i}\,(\rho_1-q_1-v_1)}-1}{\mathrm{i}\,(\rho_1-q_1-v_1)}, \quad (80)$$

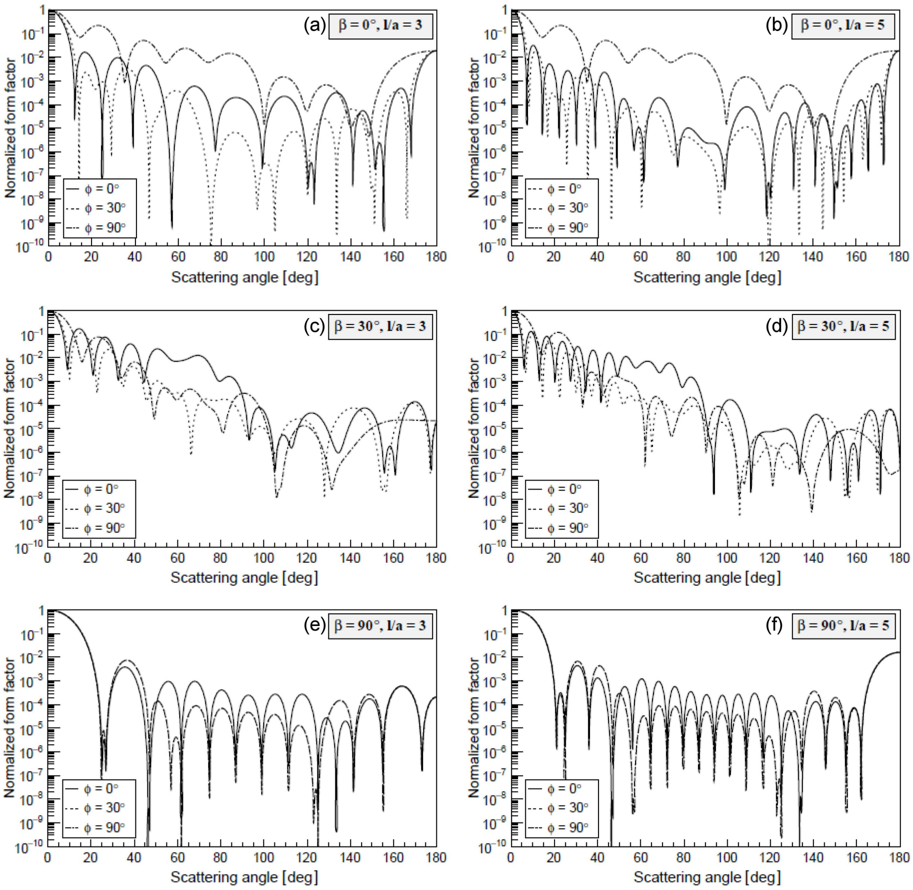

Fig. 4. Normalized form factor versus scattering angle θ for hexagonal particle at a wavelength $\lambda = 0.55$ μm with refractive index $m = 1.311 + \mathrm{i}0.31 \times 10^{-8}$ and for $\frac{l}{a} = 3$ and $\frac{l}{a} = 5$.

$$b_1 = \tfrac{a}{2}\,\mathrm{e}^{\mathrm{i}\,2v_1}\,\frac{\mathrm{e}^{-\mathrm{i}\,(q_1+v_1)} - 1}{(-\mathrm{i})\,(q_1+v_1)}, \tag{81}$$

$$d_1 = \tfrac{a}{2}\,\mathrm{e}^{\mathrm{i}\,2v_1}\,\frac{\mathrm{e}^{\mathrm{i}\,(u_1+q_1-v_1)} - 1}{\mathrm{i}\,(u_1+q_1-v_1)}, \tag{82}$$

$$e_1 = \tfrac{a}{2}\,\mathrm{e}^{\mathrm{i}\,2v_1}\,\frac{\mathrm{e}^{\mathrm{i}\,(q_1-v_1)} - 1}{\mathrm{i}\,(q_1-v_1)}, \tag{83}$$

$$a_1^1 = \frac{l\cot(\beta)}{2\sqrt{3}}\,\mathrm{e}^{\mathrm{i}\,2v_1}\,\frac{\mathrm{e}^{\mathrm{i}\,(\rho_1'-q_1'-v_1')} - 1}{\mathrm{i}(\rho_1'-q_1'-v_1')}, \tag{84}$$

$$b_1^1 = \frac{l\cot(\beta)}{2\sqrt{3}}\,\mathrm{e}^{\mathrm{i}\,2v_1}\,\frac{\mathrm{e}^{-\mathrm{i}\,(q_1'+v_1')} - 1}{(-\mathrm{i})(q_1'+v_1')}, \tag{85}$$

$$d_1^1 = \frac{l\cot(\beta)}{2\sqrt{3}}\,\mathrm{e}^{\mathrm{i}\,2v_1}\,\frac{\mathrm{e}^{\mathrm{i}\,(u_1'+q_1'-v_1')} - 1}{\mathrm{i}(u_1'+q_1'-v_1')}, \tag{86}$$

$$e_1^1 = \frac{l\cot(\beta)}{2\sqrt{3}}\,\mathrm{e}^{\mathrm{i}\,2v_1}\,\frac{\mathrm{e}^{\mathrm{i}\,(q_1'-v_1')} - 1}{\mathrm{i}(q_1'-v_1')}, \tag{87}$$

$$a_1^2 = \tfrac{a}{2}\left(1 - \frac{l\cot(\beta)}{a\sqrt{3}}\right)\mathrm{e}^{\mathrm{i}\,(q_1+v_1)} \times \frac{\mathrm{e}^{-\mathrm{i}\,(q_1-v_1)\left(1-\frac{l\cot(\beta)}{a\sqrt{3}}\right)} - 1}{(-\mathrm{i})(q_1-v_1)\left(1 - \frac{l\cot(\beta)}{a\sqrt{3}}\right)}, \tag{88}$$

$$b_1^2 = \tfrac{a}{2}\left(1-\frac{l\cot(\beta)}{a\sqrt{3}}\right)\mathrm{e}^{-\mathrm{i}\,(q_1-v_1)} \times \frac{\mathrm{e}^{\mathrm{i}\,(q_1+v_1)\left(1-\frac{l\cot(\beta)}{a\sqrt{3}}\right)} - 1}{\mathrm{i}\,(q_1+v_1)\left(1 - \frac{l\cot(\beta)}{a\sqrt{3}}\right)}. \tag{89}$$

The parameters ρ_1 and ρ_1' have been defined in the previous section (case of $\theta = 0$).

By replacing v_1 by $-v_1$ in the above equations, one obtains the expressions of parameters a_2, b_2, d_2, e_2, a_2^1, b_2^1, d_2^1, e_2^1, a_2^2, and b_2^2 from those of a_1, b_1, d_1, e_1, a_1^1, b_1^1, d_1^1, e_1^1, a_1^2, and b_1^2, respectively.

3. Results and discussion

In order to illustrate the analytical results, we show in Fig. 4 the behavior of the normalized form factor of horizontally oriented hexagonal columns (1D freedom) versus the scattering angle θ [deg] for three values of $\varphi = 0°$, $30°$ and $90°$, at a wavelength $\lambda = 0.55$ μm, and complex index of refraction $m = 1.311 + 0.31 \times 10^{-8}\mathrm{i}$ and $ka = 10$.

These figures show that if the value of the scattering angle is increased, the intensity of the form factor lobes decreases. We can also note that by increasing the value of the aspect ratio (l/a), the number of extremes of the light also increases for the same value of φ. So, we can conclude that the form factor for horizontally oriented ice columns depends on the aspect ratio (l/a), the scattering angle θ, the azimuth angle φ, and the orientation of the particle in space. Furthermore, it can be seen from the curves that when $\beta = \frac{\pi}{2}$, the form factor depends slightly on the azimuthally φ angle. We also remark that the backscattering is almost unnoticeable compared to the front scattering.

It is important to note that from the results obtained in this work, one can deduce some results found in [15]. Especially the analytical expression of the form factor of a hexagonal particle in the WKB approximation for two particular cases of normal incidence (i.e, flat incident light and edge-on incidence) is sufficient to give a well-defined value to the angle of orientation β. We also notice that our findings are in agreement with those found in other works already published, especially those who have studied the scattering of light by other geometric shapes of non-spherical particles in the WKB approximation, such as the cube [19], the parallelepiped [20] and the hexagon [15]. The authors of those research showed the influences of scattering angle, azimuth angle, and aspect ratio (l/a). Moreover, our result, regarding the fact that in addition to the non-spherical effect of ice crystals, the orientations of these particles are also significant to their optical properties, agrees with the work of Stephens [21], who showed the importance of the shapes and orientations of non-spherical particles in radiative transfer calculations.

4. Conclusions

An analytical formulation of the WKB method for horizontally oriented ice columns is given. We determined analytical expressions of the amplitude form factor. Only the incidence on the flat facets is considered. We showed that scattering properties of horizontally oriented ice columns, which have orientations with one degree of freedom, depend on the orientations of the particles. Furthermore, the dependence of the form factor on the aspect ratio (l/a) and on the azimuthally scattering φ angle is shown. Also, it is demonstrated that the form factor depends slightly on the azimuth angle φ when $\beta = \frac{\pi}{2}$. Finally, we note that the formalism of calculus adopted in this work cannot be applied to hexagonal ice columns, which have orientations with 2D freedom. In future work, we hope to apply the WKB method for particles that have orientations with 2D freedom.

References

[1] P.V. Hobbs, *Ice Physics*, Oxford U.P., London 1974.

[2] R. Greenler, *Rainbows, Halos, and Glories*, Cambridge University Press, Cambridge 1980.

[3] M.I. Mishchenko, L.D. Travis, D.W. Mackowski, *J. Quant. Spectrosc. Radiat. Transfer.* **55**, 535 (1996).

[4] P. Yang, K.N. Liou, *J. Opt. Soc. Am. A* **13**, 2072 (1996).

[5] M.I. Mishchenko, L.D. Travis, A.A. Lacis, *Scattering, Absorption, and Emission of Light by Small Particles*, Cambridge University Press, Cambridge 2002.

[6] S. Havemann, A.J. Baran, *J. Quant. Spectrosc. Radiat. Transfer.* **70**, 139 (2001).

[7] H.C. Van de Hulst, *Light Scattering by Small Particles*, J. Wiley, New York 1957.

[8] J.D. Klett, R.A. Sutherland, *Appl. Opt.* **31**, 373 (1992).

[9] N.V. Shepelevich, I.V. Prostakova, V.N. Lopatin, *J. Quant. Spectrosc. Radiat. Transfer.* **63**, 353 (1999).

[10] A. Belafhal, M. Ibnchaikh, K. Nassim, *J. Quant. Spectrosc. Radiat. Transfer.* **72**, 385 (2002).

[11] K.A. Shapovalov, *Int. J. Civ. Eng.* **9**, 1664 (2018).

[12] K.A. Shapovalov, *Atmos. Ocean. Opt.* **20**, 12 (2007).

[13] V.M. Rysakov, *J. Quant. Spectrosc. Radiat. Transfer.* **98**, 85 (2006).

[14] G. Frederic, *Opt. Commun.* **313**, 394 (2014).

[15] M. Ibnchaikh, R. Lamsoudi, A. Belafhal, *Opt. Quantum Electron.* **48**, 466 (2016).

[16] C.M.R. Platt, *J. Appl. Meteorol.* **17**, 482 (1978).

[17] G. Chen, P. Yang, G.W. Kattawar, M.I. Mishchenko, *J. Quant. Spectrosc. Radiat. Transfer.* **100**, 91 (2006).

[18] W. Sun, Q. Fu, *J. Quant. Spectrosc. Radiat. Transfer.* **63**, 727 (1999).

[19] R. Lamsoudi, S.E. Elbahar, M. Ibnchaikh, *Iran. J. Phys. Res.* **17**, 103 (2017).

[20] R. Lamsoudi, M. Ibnchaikh, *ARPN J. Eng. Appl. Sci.* **11**, 13580 (2016).

[21] G.L. Stephens, *J. Atmos. Sci.* **37**, 2095 (1980).